

# A Resonant Push–Pull DC–DC Converter

Shiying Yuan, Zhe Tang, Jiyun Tian and Hui Cao

**Abstract** This paper presents a novel topology of a resonant push–pull DC–DC converter. The primary side of the transformer applies a traditional two-transistor push–pull circuit structure, while the secondary side of the transformer includes a circuit of duplex windings and a LC resonant voltage-double structure. The average output voltage of the converter is four times of the voltage-double resonant capacitors. The LC resonance of the voltage-double capacitors and the secondary leakage inductors of the transformer transfers the energy from the primary side to the secondary side. The circuit adopts the strategy of fixing turn-on time and frequency modulation method. All switches and diodes can achieve ZCS (zero current switching). The paper analyses every operation mode in detail. Because of symmetrical working of the secondary upper and lower windings of the transformer, it can be transformed into two-port network to analyze the AC equivalent circuit through fundamental analysis method. And on this basis, the paper deduces the gain characteristic expression of the AC fundamental wave, plots the curve of voltage gain with different frequency ratio  $m$ , excitation inductance/leakage inductance ratio  $h$  and quality factor  $Q$  by MATLAB, and utilizes the voltage gain curve to design the circuit experimental parameters. At last, a sample converter of 20–28 V input/360 V output/rated power 400 W is built and tested. The experimental waveforms verify the correctness of the circuit and validity of the gain model. The experimental conversion efficiency indicates that the switch achieves ZCS to reduce the switching loss of existing push–pull circuit effectively and improve the conversion efficiency. The measured efficiency was 93.5% at rated load.

**Keywords** LC resonance · Push–pull · Voltage-fourfold structure  
ZCS · First harmonic analysis method

---

S. Yuan (✉) · Z. Tang · J. Tian · H. Cao  
East China Jiaotong University (ECJTU), Nanchang, China  
e-mail: 405376417@qq.com

© Springer Nature Singapore Pte Ltd. 2018  
L. Jia et al. (eds.), *Proceedings of the 3rd International Conference on Electrical and Information Technologies for Rail Transportation (EITRT) 2017*, Lecture Notes in Electrical Engineering 482, [https://doi.org/10.1007/978-981-10-7986-3\\_8](https://doi.org/10.1007/978-981-10-7986-3_8)

## 1 Introduction

The traditional push–pull circuit has the advantages of simple structure and drive circuit without isolation. The disadvantages are that the voltage stress of the switch is more than two times of the input voltage, and the switch is hard-switching. Therefore many researches on improved push–pull circuit have been continuously expanding and deepening. A scheme is a soft-switching push–pull circuit of four switches in [1]. The disadvantages are the increase of the number of switches and complex isolated driver circuit. The second scheme is a soft-switching push–pull forward circuit in [2], which achieves the zero current switching and reduces the switching loss, but the disadvantages are that an auxiliary switch which increases isolated driver circuit in the secondary side is necessary and the output filter inductor is retained. The third scheme is a soft-switching three-transistor push–pull converter. Yisheng and Qunfang [3] introduces the basic topology, and the control strategy of main and vice switches is same as two bridge arms of phase shifted full bridge circuit, turn-off currents of main switches are half than the latter, but auxiliary switch could only achieve the zero voltage switching under heavy load conditions. The fourth scheme is LC resonant soft-switching push–pull circuit. Yisheng and Changwei [4] shows that if the resonant period of the secondary LC is less than turn-on time of the switch, the secondary inductor and capacitor will be resonant in multi periods. Under the condition of changing load, the output voltage will appear alternating characteristics of voltage source and current source, and the applicable range is relatively narrow.

This paper presents a novel topology of the resonant push–pull DC–DC converter with a voltage-fourfold structure, which is different from the traditional topologies of LC [4], LCL [5] and LLC [6]. The leakage inductors of transformer as resonant inductors and series resonant capacitors consist of the voltage-double resonant structure. And the voltage-double capacitors of the secondary windings have charging and discharging process on the contrary. The output voltage is four times of the average voltage of each voltage-double capacitor, which is the origin of voltage-fourfold structure. Both of the primary switches and the secondary diodes can achieve ZCS. According to the equivalent model of the circuit based on first harmonic approximation (FHA), the three dimensional curve analysis of the voltage gain variable is performed and the circuit parameters are optimized. An experimental prototype of 400 W is made. The test results verify the feasibility of the circuit and the effectiveness of the gain model.

## 2 Operation Principle

Figure 1 is the voltage-fourfold resonant push–pull circuit. Switch  $Q_1$ ,  $Q_2$  consist of the push–pull structure.  $D_1$ ,  $D_2$  are the parasitic diodes of  $Q_1$ ,  $Q_2$ . And  $C_1$ ,  $C_2$  include the parasitic capacitors and external parallel capacitors of  $Q_1$ ,  $Q_2$ .  $C_{r1}$ ,  $C_{r2}$

are the voltage-double capacitors.  $L_{11}, L_{12}, L_{13}, L_{14}$  are leakage inductors of primary and secondary sides of the transformer. The physical reference directions are shown in Fig. 1.

Before analyzing the principle of the circuit, make the following assumptions:

1. the voltage drop of the switching devices is zero;
2. the number of turns of the transformer TX:  $N_1 = N_2 = N_3/N = N_4/N$ , Where  $N$  is the ratio;  $L_{m1} = L_{m2} = L_m = L_{m3}/N^2 = L_{m4}/N^2$ ; Leakage inductances  $L_{l1} = L_{l2} = L_l = L_{l3}/N^2 = L_{l4}/N^2$  is much less than  $L_m$ ;
3. equivalent capacitances of the two switches  $C_1 = C_2 = C$ ;
4. the voltage-double capacitances  $C_{r1} = C_{r2} = C_r$ , the average voltage is  $U_o/4$ , this is the origin of voltage-fourfold structure.

The key operational waveforms of the circuit are shown in Fig. 2. In one switching period, there are eight operation modes in voltage-fourfold resonant converter, the analysis of each mode is as follows.

- (1) Mode 1 [ $t_0 \sim t_1$ ]: charging and discharging stage of parallel capacitors of the switches

In the moment before  $t_0$ ,  $Q_2$  is turned on, the loop is  $U_i - N_2 - Q_2 - U_i$ , the reverse of the excitation current increases. The excitation current reaches the maximum value of the reverse in the moment of  $t_0$ . At the time, the secondary side has ended resonance, the resonant capacitor voltage is kept constant, the voltage of  $C_{r1}$  reaches the minimum value, the voltage of  $C_{r2}$  reaches maximum value, the resonant current is zero, the winding of the secondary side is open, the primary voltage is clamped by the secondary voltage.

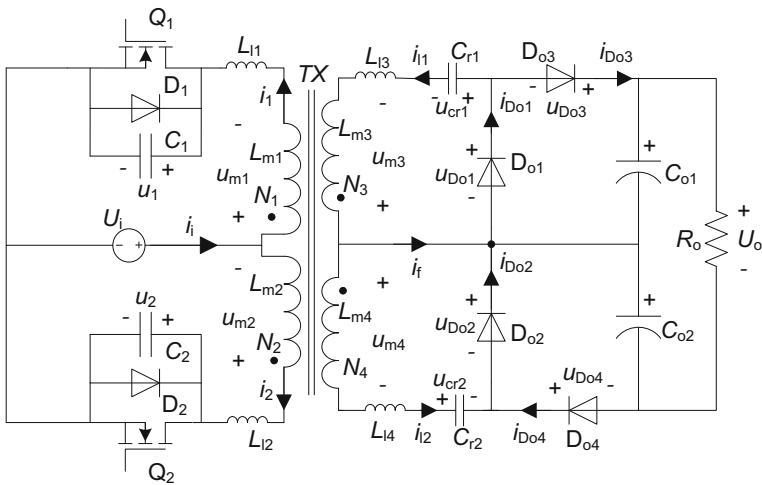


**Fig. 1** Resonant push-pull DC-DC converter with a voltage-fourfold structure

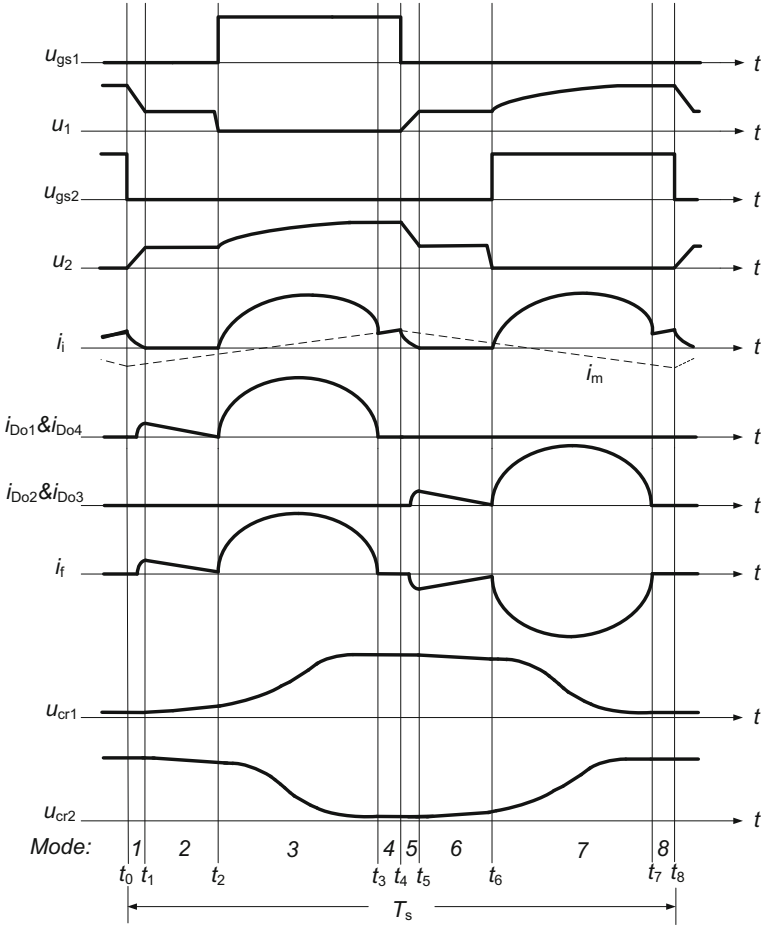


Fig. 2 Key working waveforms of the converter

In the time  $t_0$ ,  $Q_2$  is turned off, the excitation inductance and leakage inductances of the primary side and  $C_2$ ,  $C_1$  are resonant. During the resonant process, the excitation current charges  $C_2$  to make  $U_2$  rise, and discharges  $C_1$  to make  $U_1$  drop.

$U_{m2}$  has reverse reduction and then has positive increase. Set  $L_{11} = L_{12} = L_1$ , the voltage and node current equations in the primary circuit can be listed:

$$\begin{cases} U_i - u_{m1} - L_1 di_1/dt - u_1 = 0 \\ U_i + u_{m2} - L_1 di_2/dt - u_2 = 0 \\ u_{m1} = u_{m2} = u_m \\ i_1 + i_2 = i_i \\ i_2 - i_1 = I_{mm} \\ i_1 = Cdu_1/dt \\ i_2 = Cdu_2/dt \end{cases} \quad (1)$$

The variables are as follows:

$$\begin{cases} u_1 = 2U_i - I_{mm}(t - t_0)/2C + \frac{I_{mm}}{2} \sqrt{L_1/C} \sin \frac{(t-t_0)}{\sqrt{L_1C}} \\ u_2 = I_{mm}(t - t_0)/2C + \frac{I_{mm}}{2} \sqrt{L_1/C} \sin \frac{(t-t_0)}{\sqrt{L_1C}} \\ u_m = I_{mm}(t - t_0)/2C - U_i \\ i_i = I_{mm} \cos \frac{(t-t_0)}{\sqrt{L_1C}} \\ i_1 = -I_{mm}/2 + \frac{I_{mm}}{2} \cos \frac{(t-t_0)}{\sqrt{L_1C}} \\ i_2 = I_{mm}/2 + \frac{I_{mm}}{2} \cos \frac{(t-t_0)}{\sqrt{L_1C}} \end{cases} \quad (2)$$

In the formula,  $I_{mm}$  is the maximum value of the excitation current.

The leakage inductances are much less than the excitation inductance, so the leakage inductances can be neglected in series. Because this process is very short, it can be considered that the excitation current is kept constant in the process of  $I_{mm}$ .

In the time  $t_1$ ,  $u_1$  is reduced from  $2U_i$  to the platform value;  $u_2$  is increased from 0 to the platform value, and the primary voltage of the transformer rises from  $-U_i$  to the voltage valley value, which is converted from the secondary boundary value of the resonant capacitor  $C_{r1}$ . According to the solutions of the equation group, it is known that the duration of this stage is

$$t_{01} = 2C(U_{cr1} + NU_i)/NI_{mm} \quad (3)$$

(2) Mode 2 [ $t_1 \sim t_2$ ]: resonant stage of the secondary excitation

At the moment  $t_1$ , due to the rise of the voltage of  $C_2$ , the voltage of  $L_{m2}$  rises. When meeting  $u_{m3} > u_{cr1}$ ,  $u_{m4} > U_o/2 - u_{crm}$ ,  $D_{o1}$ ,  $D_{o4}$  are turned on. In the formula,  $u_{cr1}$  is the voltage valley value of the resonant capacitor  $C_{r1}$ , and  $u_{crm}$  is the voltage peak value of the resonant capacitor  $C_{r2}$ . Ideally, according to the symmetry of the circuit, the voltage valley value of the resonant capacitor  $C_{r2}$  is  $u_{cr1}$ , and the peak value of the resonant capacitor  $C_{r1}$  is  $u_{crm}$ .

Therefore, the excitation current is transferred from the primary side to the secondary side, which provides a resonant current for the secondary side. The secondary side begins to resonate, when ignoring the leakage inductors, the resonant loops are  $N_3 - D_{o1} - C_{r1} - N_3$  and  $N_4 - C_{o2} - D_{o4} - C_{r2} - N_4$ . The resonant voltage of  $C_{r1}$  rises, the resonant voltage of  $C_{r2}$  decreases, the both resonant currents decrease. The primary voltage is clamped by the secondary side.  $C_1$ ,  $C_2$ ,  $L_{11}$ ,  $L_{12}$  participate in the resonance, and each current is rapidly reduced to zero due to damping resonance. The voltage and current equations of the two top and bottom winding loops are listed as follows:

$$\begin{cases} L_{m3} di_{D_{o1}}/dt + u_{cr1} = 0 \\ i_{D_{o1}} = C_{r1} du_{cr1}/dt \\ L_{m4} di_{D_{o4}}/dt + U_o/2 - u_{cr2} = 0 \\ i_{D_{o4}} = -C_{r2} du_{cr2}/dt \\ u_{m3} = u_{m4} \end{cases} \quad (4)$$

The variables are as follows:

$$\left\{ \begin{array}{l} i_{D_{o1}} = -\frac{U_{cr1}}{N\sqrt{L_m/C_r}} \sin \omega_c(t-t_1) + \frac{I_{mm}}{N} \cos \omega_c(t-t_1) \\ u_{cr1} = I_{mm} \sqrt{L_m/C_r} \sin \omega_c(t-t_1) + U_{cr1} \cos \omega_c(t-t_1) \\ i_{D_{o4}} = \frac{U_o/2 - U_{crm}}{N\sqrt{L_m/C_r}} \sin \omega_c(t-t_1) + \frac{I_{mm}}{N} \cos \omega_c(t-t_1) \\ u_{cr2} = \frac{U_o}{2} - I_{mm} \sqrt{\frac{L_m}{C_r}} \sin \omega_c(t-t_1) \\ \quad + (U_o/2 - U_{crm}) \cos \omega_c(t-t_1) \frac{U_o}{2} - U_{crm} = U_{cr1} \\ \omega_c = 1/(N\sqrt{L_m C_r}) \end{array} \right. \quad (5)$$

In the formula,  $\omega_c$  is resonant angle frequency of series resonant circuit for this mode. According to the solutions of the equations, the relationship between the peak value and the valley value of the resonant capacitor voltage is  $U_o/2 - U_{crm} = U_{cr1}$ . The primary winding voltage is clamped by the secondary side in  $u_{cr1}/N$ , i.e., it is clamped in  $(U_o/2 - u_{crm})/N$ , and the two are equal. The platforms of  $U_1$ ,  $U_2$  occur.

In the moment  $t_2$ ,  $i_i$  drops to zero. Output diode current  $i_{D_{o1}}$  and  $i_{D_{o4}}$  drop a value of zero or slightly greater than zero, called it  $I_{m1}$ .  $u_{cr1}$  and  $u_{cr2}$  do not change much, and  $u_{cr1}$  is made up to  $U'_{cr1}$  and  $u_{cr2}$  is made down to  $U'_{crm}$  respectively.

At the end of this mode, Q1 is turned on. The duration of this mode is determined by the dead time.

(3) Mode 3 [ $t_2 \sim t_3$ ]: the main resonant stage

In the moment  $t_2$ , Q1 is turned on. The excitation inductors and leakage inductors of the primary and secondary sides and resonant capacitors are resonant together. Secondary loops are  $N_3 - D_{o1} - C_{r1} - L_{l3} - N_3$ ,  $N_4 - C_{o2} - D_{o4} - C_{r2} - L_{l4} - N_4$ . The primary resonant current varies from zero;  $u_1$  decreases and  $u_2$  increases due to resonance. The secondary resonant current varies from zero or a slightly greater than zero. The voltage of charging  $C_{r1}$  rises; the voltage of discharging  $C_{r2}$  drops.

When the primary side is converted to the secondary side, the equations are listed as follows:

$$\left\{ \begin{array}{l} NU_i - u_{cr1} - 2N^2 L_1 di_{D_{o1}}/dt = 0 \\ i_{D_{o1}} = C_{r1} du_{cr1}/dt \\ NU_i + u_{cr2} - U_o/2 - 2N^2 L_1 di_{D_{o4}}/dt = 0 \\ i_{D_{o4}} = -C_{r2} du_{cr2}/dt \end{array} \right. \quad (6)$$

The variables are as follows:

$$\left\{ \begin{array}{l} u_{cr1} = NU_i + I_{m1} N \sqrt{2L_1/C_r} \sin \omega_r(t-t_2) - (NU_i - U'_{cr1}) \cos \omega_r(t-t_2) \\ i_{D_{o1}} = \frac{NU_i - U'_{cr1}}{N\sqrt{2L_1/C_r}} \sin \omega_r(t-t_2) + I_{m1} \cos \omega_r(t-t_2) \\ u_{cr2} = U_o/2 - NU_i - I_{m1} N \sqrt{2L_1/C_r} \sin \omega_r(t-t_2) + (NU_i + U'_{crm} - U_o/2) \cos \omega_r(t-t_2) \\ i_{D_{o4}} = \frac{NU_i + U'_{crm} - U_o/2}{N\sqrt{2L_1/C_r}} \sin \omega_r(t-t_2) + I_{m1} \cos \omega_r(t-t_2) \\ i_f = \frac{2(NU_i - U'_{cr1})}{N\sqrt{2L_1/C_r}} \sin \omega_r(t-t_2) + 2I_{m1} \cos \omega_r(t-t_2) \\ U_o/2 - U'_{crm} = U'_{cr1} \end{array} \right. \quad (7)$$

In the formula,  $\omega_r = 1/(N\sqrt{2L_1C_r})$  is resonant angle frequency of series resonant circuit for this mode.

In the moment  $t_3$ , the resonance of the secondary side ends, and the resonant current is zero. The primary current drops to the excitation current.  $U_2$  rises to a certain value;  $u_{cr1}$  rises to the maximum;  $u_{cr2}$  drops to the minimum. This mode is over, the duration of this mode is

$$t_{23} = \pi N \sqrt{2L_1C_r} \quad (8)$$

(4) Mode 4 [ $t_3 \sim t_4$ ]: the charging stage of the primary excitation inductor

In the moment  $t_3$ , the secondary resonance ends,  $u_{m1}$  is  $U_i$ . The primary excitation winding is charged, the loop is  $U_i - N_1 - Q_1 - U_i$ , the secondary current is zero. The primary current  $i_i$  is the excitation current at this stage:

$$i_i = i_m(t_3) + U_i(t - t_3)/L_m \quad (9)$$

The duration of this mode is a difference between the turn-on time of the switch and the half resonant period of the secondary side.

Four modes in the follow are similar to the first four modes, i.e., the resonant capacitors of the two secondary windings have opposite charging and discharging process. Therefore that won't be said again here.

### 3 DC Gain Characteristics of the Voltage-Fourfold Resonant Converter

The circuit uses the fixed turn-on time to adjust the switching frequency  $f_s$  to control the output voltage. In order to enable the switches and diodes to achieve ZCS,  $f_s$  should be less than the resonant frequency  $f_r$ .

In the design of the circuit, the secondary resonant network ends resonance in advance before the switch is turned off, so the switch is off at the peak of the excitation current. In order to reduce the current and the turn-off switching loss, the durations of mode 4 and mode 8 must be reduced, that is, the half resonant period is close to the turn-on time.

In addition, in mode 2 and mode 6, the excitation current is very small. After the excitation current is transferred to the secondary side, the resonant current is very small, the secondary winding inductance is very large, the energy is basically unchanged, the voltage change of the secondary resonant capacitor is very small, so the function of energy transfer of mode 2 and mode 6 is ignored.

Based on above analyses, the secondary stages of energy transfer, i.e., mode 2 and mode 6, as well as the modes which time are very short, i.e., mode 1, 4, 5, 8, are ignored. So only consider the main stages of energy transfer, namely, mode 3 and mode 7.

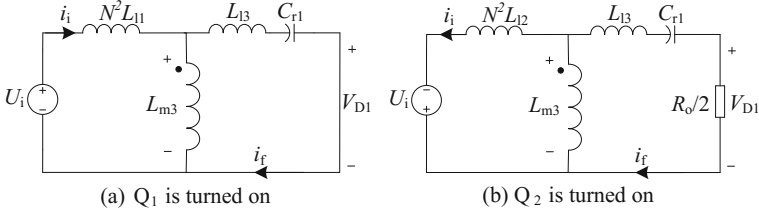


**Fig. 3** Two-port network at different switches terms

In mode 3 and mode 7, the switches  $Q_1$ ,  $Q_2$  are turned on respectively. The primary and secondary windings of the converter in essence are three-port, but due to symmetrical working of upper and lower windings, it can be transformed into two-port network to analyze the AC equivalent circuit through fundamental analysis method. The equivalent models of the two secondary windings are the same. In order to simplify the analysis, when the circuit is stable, only the equivalent model of the upper winding is analyzed.

When  $Q_1$  is turned on, the network diagram of the two-port network is shown in Fig. 3a. When  $Q_2$  is turned on, the network diagram of the two-port network is shown in Fig. 3b.

The total DC gain expression can be deduced

$$G_{dc} = \frac{U_o}{NU_i} = \frac{32mQ \sin(\pi m/2)}{\sqrt{[8mQ(H+1) \sin(\pi m/2)]^2 + \pi^4 [m^2(H+2) - 2(H+1)]^2}} \quad (10)$$

In the above formula,  $h = L_{13}/L_{m3} = L_l/L_m$  is the leakage inductance coefficient.  $Q' = R_{a1}/\sqrt{2L_{l3}/C_{r1}}$  is resonance quality factor  $Q$  is custom quality factor,  $Q = \frac{R_o/2}{\sqrt{2L_{l3}/C_r}}$ .

## 4 Design of Key Circuit Parameters

The key circuit parameters of  $m$ ,  $Q$  and  $h$  are designed by using the voltage-fourfold resonant converter of input DC voltage 20–28 V, output voltage 360 V, rated power 400 W, working frequency of  $f_s = 40$ –80 kHz as an example.

In the actual circuit, due to the line loss and other reasons, the voltage gain is not up to the highest value. Therefore, take  $G_{dc(\max)} = 3.7$  here. So the transformer ratio is

$$N = \frac{U_{o(\min)}}{U_{i(\min)} G_{dc(\max)}} = 4.86 \quad (11)$$

At the same time, according to the maximum input voltage, the required minimum voltage gain can be obtained as follows

$$G_{dc(\min)} = \frac{U_{o(\max)}}{NU_{i(\max)}} = 2.65 \quad (12)$$

Based on the total DC gain expression (10),  $Q$  is fixed to 8.3 firstly, then the leakage inductance coefficient  $h$  is desirable for 1/350. In order to ensure that the switch is turned off with a smaller current and the dead time is considered, the maximum operating frequency of the switch should be slightly less than  $f_r$ ,  $T_{\text{on}}$  is desirable for 6.2  $\mu\text{s}$ , so the resonant frequency  $f_r$  of the circuit is desirable for 81 kHz.

According to the custom quality factor  $Q$  and the resonant frequency formula of the circuit in the expression of DC voltage gain, the following equations can be listed:

$$\begin{cases} Q = \frac{R_o/2}{\sqrt{2L_{13}/C_r}} \\ f_r = \frac{1}{2\pi\sqrt{2L_{13}C_r}} \\ R_o = \frac{U_o^2}{P_o} \end{cases} \quad (13)$$

The solutions of the above equations can be obtained,  $R_o = 324 \Omega$ ,  $L_{13} = L_{14} = 19.3 \mu\text{H}$ ,  $C_{r1} = C_{r2} = C_r = 100 \text{ nF}$ , then  $L_{m3} = L_{13}/h = 6.8 \text{ mH}$ ;  $L_{m1} = L_{m3}/N^2 = 288 \mu\text{H}$ ;  $L_{11} = L_{12} = L_{13}/N^2 = 0.8 \mu\text{H}$ .

The circuit selects UC3867 as the driver chip and ETD49 as the core of the transformer. A laboratory prototype with a rated power of 400 W is made according to the above circuit parameters.

## 5 Experimental Results

Figure 4 shows the test waveforms of the input voltage of 20, 24 and 28 V respectively under rated load conditions. As can be seen from the secondary resonant current waveform in each figure, the excitation current is very small relative to the resonant current, the switch can achieve zero current shutdown; the primary current is resonant from zero, the switch achieves zero current switching; The half of the secondary resonant period is slightly less than the turn-on time of the switch, so the secondary current is resonant in advance, and the diode can achieve zero current shutdown. The switching frequency is adjusted to 77, 48 and 41 kHz.

Figure 5a shows the waveforms of the resonant capacitor voltage  $u_{cr1}$  of the secondary upper winding and the resonant current  $i_{11}$ , as well as the waveform of the diode voltage  $u_{D01}$  under the rated input/nominal load; there is no voltage spike

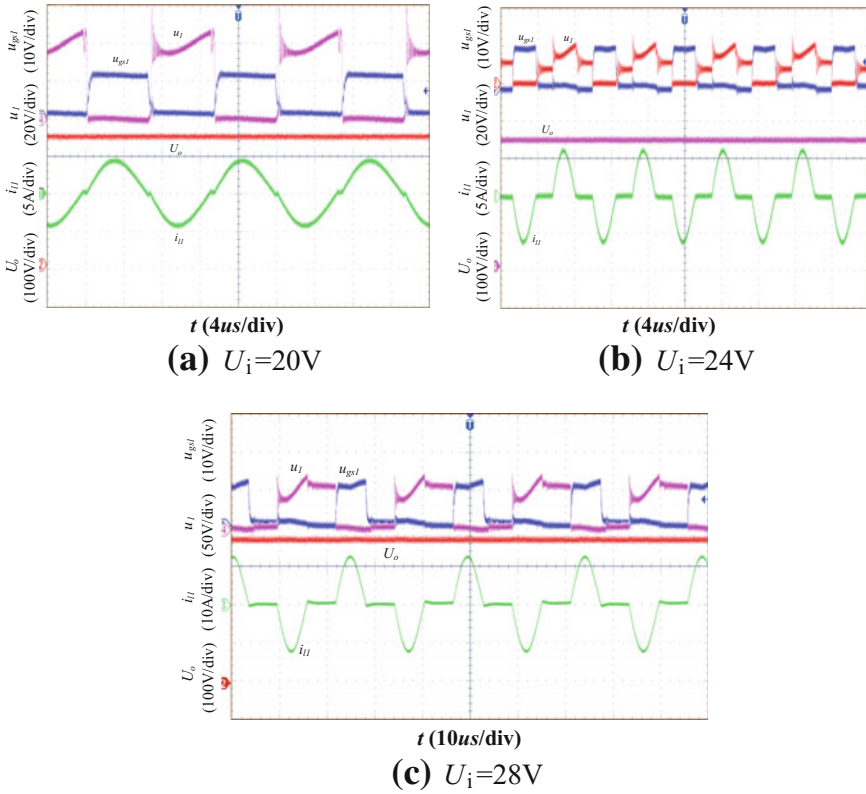


Fig. 4  $u_{gs1}$ ,  $u_t$ ,  $i_{l1}$  and  $U_o$  waveforms at different input voltage with full load

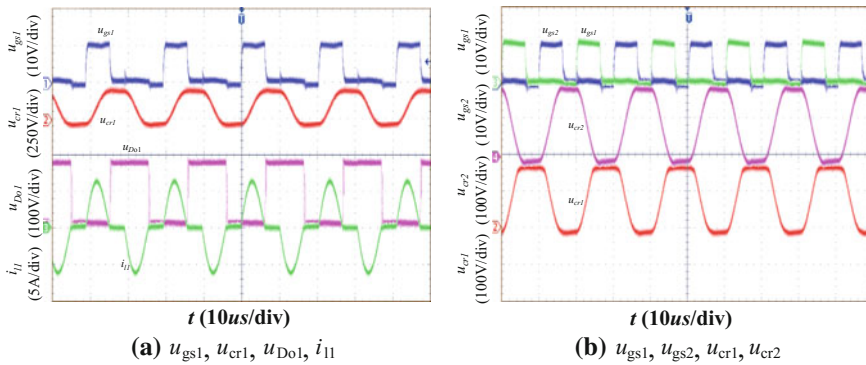


Fig. 5  $u_{gs1}$ ,  $u_{gs2}$ ,  $u_{Do1}$ ,  $i_{l1}$ ,  $u_{cr1}$  and  $u_{cr2}$  waveforms at 24 V input voltage with full load

in  $u_{D_{o1}}$  and  $u_{D_{o2}}$ , the voltage of the diode is zero in mode 2, the diode withstands reverse voltage of  $U_o/2$  in mode 6. The circuit is suitable for high voltage output.

In Fig. 5b,  $u_{cr1}$  and  $u_{cr2}$  are similar to trapezoidal wave, and the valley value can be negative, the peak value can be greater than  $U_o/2$ , but its average value is  $U_o/4$ . And the rapid change of the voltage is only in mode 3 and mode 7, which is consistent with the theoretical analysis. The rise and fall of the voltage of  $C_{r1}$  are not synchronized with those of  $C_{r2}$ , but the slopes of the rise and fall of the voltages are the same, the peak and the valley voltage of them are the same and mirror symmetrical.

The measured efficiency under the rated load is 93.5%.

## 6 Conclusion

This paper presents a topology of a resonant push–pull DC–DC converter with a voltage-fourfold structure. The circuit has the following characteristics:

1. The output voltage is 4 times of the average voltage of the voltage-double capacitor, which is voltage-fourfold structure. Its maximum voltage conversion rate is  $4N_s/N_p$ . And it is suitable for large current input and high voltage output.
2. The circuit adopts the secondary LC resonant mode. The switch can be turned on in a wide range of load with zero current and turned off with a small excitation current.
3. The voltage of each rectifier diode is only half of the output voltage. The secondary current is resonant to zero in advance during the turn-on time of the switch. The switch achieves ZCS to reduce the switching loss of existing push–pull circuit effectively and improve the conversion efficiency.
4. Different from the traditional frequency conversion mode, the circuit adopts the frequency conversion mode of fixed conduction time, which makes the result of the fundamental analysis method more accurate and effective.

**Acknowledgements** This work is partially supported by the National Natural Science Foundation of China (No.51467005), the Key Research and Development Plan of Jiangxi Province (20171BBE50018), and the foundation of East China Jiaotong University (No. 14DQ02).

## References

1. Yundong M, Linquan M, Xinbo R et al (2006) Zero-voltage-switching PWM push–pull three-level converter. Proc CSEE 26(23):36–41 (in Chinese)
2. Fanghua Z, Huizhen W, Yangguang Y (2003) ZCS scheme of push–pull forward converter. Power Electron 37(2):60–62 (in Chinese)
3. Yisheng Y, Qunfang W (2012) ZVS three-transistor push–pull DC/DC converter. Proc CSEE 32(33):23–30 (in Chinese)

4. Yisheng Y, Changwei G (2012) Resonant push-pull DC-DC converter. *Electr Power Autom Equip* 32(10):83-87
5. Quanming L, Can Z, Shubo Z, Guohui L, Luowei Z (2013) Constant current LED driver based on LCL-T half bridge resonant converter. *Trans China Electro-technical Soc* 28(12):320-323
6. Haibing H, Wanbo W, Wenjin S, Shun D, Yan X (2013) Optimal efficiency design of LLC resonant converters. *Proc CSAEE* 33(18):48-56